

The SUSY Yang-Mills plasma in a T -matrix approach

Gwendolyn Lacroix* and Claude Semay†

*Service de Physique Nucléaire et Subnucléaire,
Université de Mons – UMONS, Place du Parc 20, 7000 Mons, Belgium*

Fabien Buisseret‡

*Service de Physique Nucléaire et Subnucléaire,
Université de Mons – UMONS, Place du Parc 20, 7000 Mons, Belgium;
Haute École Louvain en Hainaut (HELHa),
Chaussée de Binche 159, 7000 Mons, Belgium*

(Dated: June 8, 2019)

Abstract

The deconfined phase of $\mathcal{N} = 1$ supersymmetric Yang-Mills theory is studied within a T -matrix formulation in the temperature range $(1-5) T_c$, where the medium is expected to be strongly coupled. Binary bound states of gluons and gluinos are found to be bound up to $1.3 T_c$. Then, the pressure and trace anomaly are computed for $SU(N)$ gauge groups. The orientifold duality and its accuracy at $N = 3$ is finally discussed.

* E-mail: gwendolyn.lacroix@umons.ac.be

† E-mail: claude.semay@umons.ac.be

‡ E-mail: fabien.buisseret@umons.ac.be

I. INTRODUCTION

The phenomenology related to the QCD confinement/deconfinement phase transition has been the subject of intense investigation, both experimentally and theoretically (see *e.g.* [1] for a review of the topic). In comparison to QCD however, less information is known about the finite-temperature behavior of generic Yang-Mills (YM) theories, *i.e.* with an other gauge group than $SU(3)$ and matter in other representations than the fundamental one. Several results about a pure YM theory can be mentioned. First, there still exists a first-order deconfining phase transition with the gauge groups G_2 , $SU(N > 3)$, $SP(2)$ and E_7 [2–4]. Second, the equation of state (EoS) above the deconfining temperature T_c , appears to be nearly independent of the gauge group once normalized to the Stefan-Boltzmann pressure [4, 5]. Below T_c , the EoS seems to be compatible with a Hagedorn-type density of state with the Hagedorn temperature playing the role of T_c [6, 7].

Among other extensions of YM theories, a particularly challenging case is the one with one flavor of massless Majorana fermions in the adjoint representation of the gauge group. Such a theory is supersymmetric and is the $\mathcal{N} = 1$ SUSY YM theory [8], the adjoint quarks being called the gluinos. As in ordinary YM theory, the behavior of $\mathcal{N} = 1$ SUSY YM theory can be guessed from the β -function. It has been exactly computed from instanton calculus [9], and reads $\beta(g) = -\frac{g^3}{16\pi^2} \frac{3N}{1 - \frac{g^2 N}{8\pi^2}}$ for an $SU(N)$ gauge group. This form is compatible with asymptotic freedom, and it appears that $\mathcal{N} = 1$ SUSY YM is confining at $T = 0$, as in the ordinary YM case. Several studies have been thus devoted to compute its spectrum with the gauge groups $SU(N)$ [10–15]. Moreover, the theory is expected to exhibit a deconfining phase transition: Recent lattice results indicate that it is indeed the case, at least for $SU(2)$ [16]. This might be the case for an arbitrary gauge group too, according to [17]. At very high temperatures finally, the deconfined phase is expected to behave as a conformal gas of gluons and gluinos [18].

A peculiarity of $SU(N)$ $\mathcal{N} = 1$ SUSY YM is that it is equivalent to one-flavor QCD at large N provided that quarks are in the two-indices antisymmetric representation of the gauge group, which is isomorphic to the fundamental one at $N = 3$. This duality is called orientifold duality and has attracted a lot of attention since the pioneering work [19].

The aim of the present work is to study the thermodynamic features of the deconfined phase of $\mathcal{N} = 1$ SUSY YM theory by resorting to the formalism described in [5]. This

formalism is based on a T -matrix approach that allows to model the bound states and scattering states of the system in a unified way [20]. From the T -matrix, the EoS can be computed by resorting to the Dashen, Ma and Bernstein's formulation of statistical mechanics [21]. Such a formulation is particularly well suited for systems whose microscopic constituents behave according to relativistic quantum mechanics: In our framework, the deconfined phase is seen as a strongly interacting gas of gluons and gluinos propagating in the plasma. Note that the approach described in [5] has already proven to reproduce accurately the current lattice data concerning the EoS of ordinary YM theory for the gauge groups $SU(N)$.

The paper is organized as follows. Sec. II is a summary of the approach used here and about which detailed explanations can be found in [5]. In Sec. III, we particularize the approach to the $\mathcal{N} = 1$ SUSY YM case and compute the bound state spectrum, at $T = 0$ and above T_c . The EoS of the deconfined phase is then presented in Sec. IV for the gauge group $SU(N)$. In Sec. V we show that our approach is compatible with the aforementioned orientifold equivalence. Our results are finally summarized in Sec. VI, while technical details are given in the Appendices.

II. T -MATRIX FORMALISM IN STATISTICAL PHYSICS

A. Generalities

The results of Ma, Dashen and Bernstein [21] establishing the grand potential of an interacting relativistic particle gas, Ω , expressed as an energy density, are summarized by the following virial expansion (in units where $\hbar = c = k_B = 1$).

$$\Omega = \Omega_0 + \sum_{\nu} \left[\Omega_{\nu} - \frac{e^{\beta \vec{\mu} \cdot \vec{N}}}{2\pi^2 \beta^2} \int_{M_{\nu}}^{\infty} \frac{d\epsilon}{4\pi i} \epsilon^2 K_2(\beta \epsilon) \text{Tr}_{\nu} \left(\mathcal{S} S^{-1} \overleftrightarrow{\partial}_{\epsilon} S \right) \Big|_c \right]. \quad (1)$$

In this equation, the first term, Ω_0 , is the grand potential of the free relativistic particles. The second term accounts for interactions in the plasma and is a sum running on all the species, the number of particles included, and the quantum numbers necessary to fix a channel. The set of all these channels is generically denoted ν . The vectors $\vec{\mu} = (\mu_1, \mu_2, \dots)$ and $\vec{N} = (N_1, N_2, \dots)$ contain the chemical potentials and the particle number of each species taking part in a given scattering channel.

In (1), we can notice that the contribution of the bound states and scattering states are decoupled. Below the threshold M_ν (the threshold is a summation on the mass of all the particles included in a given channel ν), bound states appearing in the S -matrix spectrum are added as free additional species: Ω_ν is the grand canonical potential describing an ideal relativistic gas of the ν -channel bound states. Above M_ν , the scattering contribution is expressed as an integration depending on a trace, taken in the center of mass frame of the particles in the channel ν , and is a function of the S -matrix, S , of the system. S is in particular a function of the total energy ϵ . The symmetrizer \mathcal{S} enforces the Pauli principle when a channel involving identical particles is considered, and the subscript c means that only the connected scattering diagrams are taken into account. $K_2(x)$ is the modified Bessel function of the second kind and $\beta = 1/T$ where T is the temperature. The notation $A \overleftrightarrow{\partial}_x B$ denotes $A(\partial_x B) - (\partial_x A)B$.

By definition, S is linked to the off-shell T -matrix, \mathcal{T} , by the relation

$$S = 1 - 2\pi i \delta(\epsilon - H_0) \mathcal{T}, \quad (2)$$

where H_0 is the free Hamiltonian of the system. A way to obtain \mathcal{T} is to solve the Lippmann-Schwinger equation, schematically given by

$$\mathcal{T} = V + V G_0 \mathcal{T}, \quad (3)$$

with G_0 the free propagator and V the interaction potential. Once Eq. (1) is computed, all thermodynamic observables can be derived. For example, the pressure is simply given by

$$p = -\Omega. \quad (4)$$

The sum \sum_ν appearing in (1) explicitly reads $\sum_n \sum_I \sum_{J^{PC}} \sum_{\mathcal{C}}$, where $n \geq 2$ is the number of particles involved in the interaction process, I is a possible isospin channel, \mathcal{C} is the color channel, and J^{PC} is the spin/helicity channel (the labels C or P must be dropped off if the charge conjugation or the parity are not defined). As in [5], we assume that the dominant scattering processes are the two-body ones, and thus we only consider $n = 2$.

B. Quasiparticle properties

A key ingredient of the present approach is the 2-body potential V , encoding the interactions between the particles in the plasma. V is chosen as in [5]: It is extracted from

the free energy F_1 between a $q\bar{q}$ pair at finite temperature computed in quenched SU(3) lQCD [22]. For the needs of our approach, this free energy has been fitted with a Cornell potential screened thanks to the Debye-Hückel theory [23] (see Appendix B in [5]). However as in [5], we prefer to use the internal energy as the interaction potential. This choice is still a matter of debate. Nevertheless, it has given correct results in the ordinary YM case, as shown in [5]. After having computed the internal energy U_1 , the one-gluon exchange color dependence is used to extract the leading-order gauge group dependence of the lattice $q\bar{q}$ -potential, $U_1(r, T)$ for $T > T_c$, as proposed in Sec. II in [5]. Finally, we arrive to the following form:

$$V(r, T) = \frac{\kappa_{\mathcal{C};ij}}{\kappa_{\mathcal{C};q\bar{q}}} [U_1(r, T) - U_1(\infty, T)], \quad (5)$$

where

$$\kappa_{\mathcal{C};ij} = \frac{C_2^{\mathcal{C}} - C_2^{R_i} - C_2^{R_j}}{2C_2^{\text{adj}}}, \quad (6)$$

and where C_2^R is the quadratic Casimir of the representation R . \mathcal{C} , adj, R_i and R_j stand respectively for the pair, adjoint, i - and j -particle representation. For instance,

$$C_2^{\text{adj}} = N, C_2^\bullet = 0, C_2^q = C_2^{\bar{q}} = \frac{N^2 - 1}{2N}, \quad (7)$$

for the SU(N) gauge group (the singlet representation is denoted by \bullet). The values taken by (6) for the various color channels considered in this paper are given in Tables III-VI in Appendix A. Let us note that $\kappa_{\mathcal{C};q\bar{q}} = -4/9$ in this work, since $U_1(r, T)$ is fitted on a singlet $q\bar{q}$ potential for SU(3) [5].

In (5), the long-distance behavior of the lattice potential $U_1(\infty, T)$, is subtracted since this term is assimilated, as suggested in [24], as a thermal mass contribution for the quasiparticles (this also ensures the convergence of the scattering equation and the possibility to perform the Fourier transform). Indeed, when the quasiparticles are infinitely separated, the only remaining potential energy can be seen as a manifestation of the in-medium self-energy effects, $U_1(\infty, T) = 2m_q(T)$. We thus encode these effects as a mass shift $\delta(T)$ to the “bare” quasiparticle mass m_0 , by following the arguments exposed in [5]:

$$m(T)^2 = m_0^2 + \delta(T)^2, \quad (8)$$

where m_0 is independent of T . In order to get the thermal mass for any particles, we extract the first-order color dependence in agreement with the hard-thermal-loop (HTL)

leading-order behavior [25]:

$$\delta(T) = \sqrt{\frac{C_2^R}{C_2^{\text{adj}}}} \Delta(T), \quad (9)$$

where the quantity $\Delta(T)$ is assumed to be color-independent. As $U_1(r, T)$ is fitted on a singlet $q\bar{q}$ potential for SU(3), we have here

$$\frac{U_1(\infty, T)}{2} = m_q(T) = \sqrt{\frac{C_2^q}{C_2^{\text{adj}}}} \Delta(T) = \frac{2}{3} \Delta(T). \quad (10)$$

In particular, $\delta(T) = \Delta(T)$ for the gluon and the gluino since they both belong to the adjoint representation of the gauge group. It comes naturally that $\delta(T)$ for these particles is gauge-group independent in our model. Comments about the behavior of $m(T)$ can be found in Sec. V in [5].

C. Solving Lippman-Schwinger equations

Having established the quasiparticle properties, we have now all the ingredients to solve the Lippman-Schwinger equation leading to the on-shell T -matrix. It can be computed from (3) as follows in [5]:

$$\begin{aligned} \mathcal{T}_\nu(E; q, q') &= V_\nu(q, q') + \frac{1}{8\pi^3} \int_0^\infty dk k^2 V_\nu(q, k) \\ &\times G_0(E; k) \mathcal{T}_\nu(E; k, q') [1 \pm f_{p_1}(\epsilon_1)] [1 \pm f_{p_2}(\epsilon_2)], \end{aligned} \quad (11)$$

where E is the energy in the center-of-mass frame, ϵ_i the asymptotic energy of the particle i , and where the free two-body propagator is given by (C3). The symbol ν stands for the particular channel considered.

For ordinary $|^{2S+1}L_J\rangle$ states, $V_\nu(q, q')$ is given by the Fourier transform of the interaction

$$V_L(q, q') = 2\pi \int_{-1}^{+1} dx P_L(x) V(q, q', x), \quad (12)$$

where P_L is the Legendre polynomial of order L , and $x = \cos \theta_{q, q'}$ with $\theta_{q, q'}$ the angle between the momenta \vec{q} and \vec{q}' . The spin S is not indicated since our interaction is spin-independent. Our potential has a spherical symmetry. We have then

$$V(q, q', \theta_{q, q'}) = 4\pi \int_0^\infty dr r V(r) \frac{\sin(Q r)}{Q}, \quad (13)$$

where $Q = \sqrt{q^2 + q'^2 - 2qq' \cos \theta_{q, q'}}$.

When at least one particle is transverse, we have to use the helicity formalism [26]. It is very convenient to use, since a particular helicity state $|J^P\rangle$ can be written as (see Appendix B)

$$|J^P\rangle = \sum_{L,S} C_{L,S} |^{2S+1}L_J\rangle. \quad (14)$$

Then, it can be shown that

$$V_{J^P}(q, q') = \sum_{L,S} C_{L,S}^2 V_L(q, q'), \quad (15)$$

since our interaction is spin-independent.

Contrary to the T -matrix equation used in [5], we have included the in-medium effects, namely the Bose-enhancement and the Pauli-blocking. According to [27], these in-medium effects change the cross-section as follows,

$$\sigma^{med} = \sigma^{vac}(1 \pm f_{p_1})(1 \pm f_{p_2}), \quad (16)$$

where σ^{vac} and σ^{med} are respectively the cross-section in the vacuum and in the medium, and where f_p is the distribution function of the p -species. If the species is a boson,

$$f_p(\epsilon) = \frac{1}{e^{\beta(\epsilon-\mu)} - 1}, \quad (17)$$

while if the species is a fermion,

$$f_p(\epsilon) = \frac{1}{e^{\beta(\epsilon-\mu)} + 1}, \quad (18)$$

where μ is a possible chemical potential. The sign choice in (16) also depends on the nature of the particles: $+$ for bosons and $-$ for fermions. Let us note that these in-medium effects have a very small influence on the EoS in our computations. Therefore, the results obtained in [5] remain valid.

The Haftel-Tabakin algorithm is used to solve (11) [28]. The momentum integral is discretized within an appropriate quadrature, thus turning the integral equation in a matrix equation, namely, $\sum \mathcal{F}_{ik} \mathcal{T}_{kj} = V_{ij}$, where, schematically [20],

$$\mathcal{F} = 1 - wVG(1 \pm f_{p_1})(1 \pm f_{p_2}) \quad (19)$$

and w denotes the integration weight. The solution follows trivially by matrix inversion. It can be shown that the determinant of the transition function \mathcal{F} (referred to as the Fredholm

determinant) vanishes at the bound state energies, which provides a numerical criterion for solving the bound state problem. This strategy has already been successfully used to compute T -matrices in [5, 20]. Once $\mathcal{T}(E; q, q')$ is known, the on-shell T -matrix is readily obtained as $\mathcal{T}(E; q(E), q(E))$, with $q(E)$ given by (C1).

D. Computing the equation of state

The first term in (1) is the free relativistic gas. It is given by

$$\Omega_0 = \sum_{\text{species}} (2I + 1) \times \dim J \times \dim \mathcal{C} \times \omega_{\pm}(m). \quad (20)$$

The sum runs on each species inside the plasma. I is the isospin of the particle, $\dim J$ is the dimension of the spin/helicity representation, and $\dim \mathcal{C}$ is the dimension of the color representation. Moreover,

$$\omega_+(m) = \frac{1}{2\pi^2\beta} \int_0^\infty dk k^2 \ln \left(1 - e^{-\beta\sqrt{k^2+m^2}} \right) \quad (21)$$

is the grand potential per degree of freedom associated to a bosonic species with mass m , while

$$\omega_-(m) = -\frac{1}{2\pi^2\beta} \int_0^\infty dk k^2 \ln \left(1 + e^{-\beta\sqrt{k^2+m^2}} \right) \quad (22)$$

is the grand potential per degree of freedom associated to a fermionic species with mass m . For later convenience, the thermodynamic quantities will be normalized to the Stefan-Boltzmann pressure, which is defined as

$$p_{SB} = - \lim_{m \rightarrow 0} \Omega_0. \quad (23)$$

Attractive interactions in a particular channel ν can lead to the formation of bound states with masses $\mu_\nu < m_1 + m_2$. As mentioned above, the energy of these states can be computed by looking at the zeros of the determinant of the transition function \mathcal{F} . They contribute also to the grand potential as new species via the formula

$$\sum_{\nu} \Omega_{\nu} = \sum_{\text{attractive channels}} (2I_{\nu} + 1) \times (2J_{\nu} + 1) \times \dim \mathcal{C}_{\nu} \times \omega_{\pm}(\mu_{\nu}). \quad (24)$$

In this sum, $\omega_{\pm}(\mu_{\nu}) = 0$ if no bound state exists in the channel ν at a given value of T . The full form of the scattering part of (1) is given in Appendix C and is not recalled here for the sake of clarity.

For obvious numerical reasons, all the possible channels contributing to Ω can not be included into the sum (1). So we need reliable criteria to select the most significant channels. When the total spin J increases, the average value $\langle \vec{L}^2 \rangle$ increases also. This is obvious for ordinary spin states, and this is shown in Appendix B for helicity states. For a bound state, this means the increase of the mass, and then a reduced contribution to the grand potential. Moreover, in a naive nonrelativistic picture, the strength of the orbital barrier increases with $\langle \vec{L}^2 \rangle$ in a scattering process, which reduces the value of the corresponding T -matrix (11) (see Appendix D). So we decided to restrict the sum (1) to channels with the lowest values of $\langle \vec{L}^2 \rangle$. More precisely, a mean cross section $\bar{\sigma}_{JP}$ is computed for each channel (see Appendix D). Are only retained, the channels for which the value of $\bar{\sigma}_{JP}$ is at least 25% of the value $\bar{\sigma}_{JP}$ for the channel with the lowest value of $\langle \vec{L}^2 \rangle$. In this case, nearly all states with $\langle \vec{L}^2 \rangle \leq 5$ are retained in the sum.

E. $T = 0$ bound states

With the formalism described above, it is possible to compute bound states within the plasma (see Sec. II C). Nevertheless, it is also interesting to compute bound states at $T = 0$, in order to check the validity of our model. In quenched SU(3) lattice QCD, the potential between a static quark-antiquark pair at zero temperature is compatible with the funnel form [29]

$$V_f(r) = \sigma r - \frac{4}{3} \frac{\alpha}{r}, \quad (25)$$

where $\alpha \sim 0.4$ and $\sigma \sim 0.2 \text{ GeV}^2$ (standard values for the running coupling constant α and the string tension σ at $T = 0$). Since the Fourier transform of $V_f(r)$ is not defined (because of a nonzero asymptotic value), a string-breaking value, V_{sb} , is introduced to make it convergent. V_{sb} is thus seen as the energy above which a light quark-antiquark pair can be created from the vacuum and breaks the QCD string. This scale is then subtracted and the potential effectively taken into account is $V_f(r) - V_{sb}$, while $V_{sb}/2$ is interpreted as an effective quark mass using the same arguments as those detailed in Sec. II B.

According to the color scaling (6), the potential describing the interactions between two color sources (with representations R and \bar{R}) at zero temperature, and thus only in a singlet

gauge representation ($C_2^\bullet = 0$) since confinement is present, is

$$V_0(r) = \frac{9}{4} \left(C_2^R + C_2^{\bar{R}} \right) V_f(r) - V_{sb}^R. \quad (26)$$

Let us recall that the factor $9/4$ appears since the potential V_f is fitted on a singlet $q\bar{q}$ pair for $SU(3)$. In this case, V_{sb}^R should rather be interpreted as the energy scale necessary to form two sources of color compatible with the existence of the two new color singlet pairs of particles created by the string breaking. For instance, it is expected that two gluelumps can be formed for the breaking of a string between two gluons (a gluelump is a gluon bound in the color field of a static adjoint source). If m_0 is the bare mass of the particle, the $T = 0$ mass $m(0)$ used to compute the bound state is then

$$m(0)^2 = m_0^2 + \left(\frac{V_{sb}^R}{2} \right)^2, \quad (27)$$

keeping the same structure as in (8). This procedure is the same as the one used in [5].

III. BOUND STATES IN $\mathcal{N} = 1$ SUSY YM

Now, we will particularize the general formalism presented in the previous section for an $\mathcal{N} = 1$ SUSY YM theory with gauge group $SU(N)$. In such a theory there are two species of quasiparticles: the gluons (g) and their supersymmetric partners, the gluinos (\tilde{g}). Both particles have a vanishing isospin. Note that the nonsupersymmetric case was treated in [5]. The gluons are transverse spin-1 bosons in the adjoint representation of the gauge group and thus, since the gluinos are their supersymmetric partners, they are Majorana fermions of spin $1/2$ belonging to the same representation. The two-body channels to be considered are gg , $\tilde{g}\tilde{g}$ and $g\tilde{g}$. The lowest corresponding spin/helicity states are given in Appendix B, and the possible color channels can be found in Appendix A.

Unbroken supersymmetry is assumed in this paper, so the parameters can be fixed assuming that $m_g = m_{\tilde{g}}$ (so, $m_{0g} = m_{0\tilde{g}} = m_0$) and the interaction potential is the one used in [5], independent of the interacting species, gluon or gluino. So, in this reference, we have $m_0 = 0.7$ GeV, $T_c = 0.3$ GeV, $\sigma = 0.176$ GeV², and $\alpha = 0.4$ for $T = 0$, while $\alpha = 0.141$ for $T > T_c$. Note that T_c might be approximately 20% lower in the case under study than in ordinary YM theory [16], but such fine corrections will not be investigated here, where we aim at a first study of the topic. The value for m_0 was obtained in [5] by reproducing

the lattice light-glueball spectrum at $T = 0$. Moreover, it is an acceptable value for the zero-momentum limit of the gluon propagator at $T = 0$, see e.g. Refs. [30–32].

As explained in [5], T_c and m_0 are assumed to be gauge-group-independent. With the value chosen for the parameters, $T_c/\sqrt{\sigma} = 0.72$, which is very close to the ratio 0.69 expected from the Hagedorn spectrum in the non SUSY case [6, 7]. Actually, $\sqrt{\sigma}$ can be taken as the fundamental scale of energy, so that the meaningful parameters are $m_0/\sqrt{\sigma}$ and $T_c/\sqrt{\sigma}$.

A. Zero temperature

The zero temperature spectrum of the theory can be computed by solving (11) with potential (26). Although our main goal is the study of the deconfined phase of the theory, computing the zero temperature spectrum has an interest in view of comparing with current lattice data. Our results are given in Table I for the lightest two-body bound states we find in the singlet channel. Note that, in our formalism, these masses are independent of the number of colors, as already shown in [5]. Some degeneracies are due to the fact that our potential is spin-independent.

TABLE I. Masses (in GeV) of the lowest-lying bound states at $T = 0$ with the gauge group $SU(N)$ in $\mathcal{N} = 1$ SUSY YM. J^{PC} is indicated for gg and $\tilde{g}\tilde{g}$ states. The notation defined in Appendix B is used to further characterize the $\tilde{g}g$ states, although parity is meaningless in this case.

Content	State	Mass
$\tilde{g}\tilde{g}$	0^{-+}	1.58
	$\{0, 1, 2\}^{++}$	2.26
$\tilde{g}g$	$\frac{1}{2}^{-}$	1.96
	$\frac{3}{2}^{-}$	2.13
	$\frac{1}{2}^{+}$	2.26
	$\frac{3}{2}^{+}$	2.31
gg	0^{++}	1.96
	2^{++}	2.21
	0^{-+}	2.26

A clear feature of our results is that the lowest-lying state is the pseudoscalar $\tilde{g}\tilde{g}$ state,

also known as the $a - \eta'$ (the adjoint η'). This conclusion is shared by all the studies we found about the topic [10–15]. Then, we find a scalar glueball degenerate with the lightest $J = 1/2$ $\tilde{g}g$ bound state. In the lattice studies [12, 14, 15], these states also follow the $a - \eta'$ but are not degenerate, although very close up to the error bars. For example, the scalar glueball is found to have a mass of 1319(120) MeV in [15], while the lightest $\tilde{g}g$ state has a mass of 1091(62) MeV. It has to be noted that our formalism does not include hyperfine splitting terms as spin-spin or spin-orbit contributions, that could lift some degeneracies in the spectrum. On the lattice side, smaller lattice sizes would be needed in order to draw definitive conclusions on the structure of the spectrum [15], so the agreement between our model and the lattice data should be, in our opinion, restricted to qualitative considerations.

B. Above T_c

The existence or not of bound states in the deconfined phase is not forbidden in principle, especially around T_c where interactions are strong enough to bind two or more particles. Within our formalism, the channels in which bound states are favored at most should contain an S -wave component to avoid the centrifugal barrier and should have a symmetry that allows the state to be in a color singlet, the color channel in which the interactions are maximally attractive.

In the gg case there are two such states: The 0^{++} and 2^{++} color singlets, corresponding to the scalar and tensor glueballs respectively. We have observed in [5] that both the scalar and tensor glueball masses at $1.05 T_c$ were compatible with the zero-temperature ones. Moreover the scalar glueball exists as a bound state up to $1.25 T_c$ while the tensor one is bound up to $1.15 T_c$. These results are independent of the number of colors and are still valid in the supersymmetric extension that we study in the present paper, since the influence of the Bose-enhancement appears very small.

The $\tilde{g}\tilde{g}$ case appears to be promising to find bound states because the 0^{-+} channel is a pure S -wave that can exist in the singlet, the $a - \eta'$. As in the glueball case, the $a - \eta'$ has a mass close to its zero temperature value in $1.05 T_c$. It survives as a bound state up to $1.30 T_c$; it is actually the most strongly bound state within our framework. The $a - \eta'$ can also exist in the symmetric adjoint color channel when the number of colors is larger than 2. This channel being less attractive, the dissociation temperature is lower and is equal to

1.20 T_c . Complete results are listed in Table II. Note that $\{0, 1, 2\}^{++}$ channels also survive at 1.05 T_c , but they disappear immediately above this temperature. That is why they are not listed in Table II.

In the $\tilde{g}g$ case, the ground state is formed in the $1/2^-$ channel. The comments that can be made are very similar to the two previous cases: The mass at 1.05 T_c is nearly equal to that at $T = 0$, and the dissociation temperature is equal to 1.25 T_c in the color singlet and to 1.10 T_c in the adjoint channel.

T/T_c	$2m_g = 2m_{\tilde{g}}$	$a - \eta' (\tilde{g}\tilde{g})$		$1/2^- (\tilde{g}g)$	
		Singlet	Adjoint ($N > 2$)	Singlet	Adjoint
1.05	2.73	1.33 / 2.67*	2.33	1.90	2.52
1.10	2.20	1.69 / -	2.09	1.92	2.16
1.15	1.98	1.74	1.96	1.87	-
1.20	1.86	1.75	-	1.82	
1.25	1.79	1.73		1.78	
1.30	1.74	1.72		-	
1.35	1.70	-			

TABLE II. Masses (GeV) of lowest-lying $\tilde{g}\tilde{g}$ and $\tilde{g}g$ states above T_c . A line mark the temperature at which a bound state is not detected anymore, and a star denotes a radial excitation below threshold. Results are valid for any N except when specified.

In summary, our computations show that two-body bound states can form in the gluino-gluon plasma for any species in the range (1-1.30) T_c . The picture developed in the pioneering work [33], where the importance of binary bound states on the features of the quark-gluon plasma was stressed, seems thus to be valid in a supersymmetric extension of YM theory too. A more detailed look at Table II shows that the behavior of a given bound state mass with the temperature is not systematic: It can either increase or decrease before dissociation. We have pointed out in [5] that the observed behavior in the glueball sector is in qualitative agreement with the lattice study [34]. As soon as gluinos are involved, there are, to our knowledge, no study to which our results can be compared.

IV. EQUATION OF STATE OF $\mathcal{N} = 1$ SUSY YM

A. Strongly coupled regime

We are now in position to compute the pressure of $\mathcal{N} = 1$ SUSY YM normalized to the Stefan-Boltzman pressure, which reads $p_{SB} = \pi^2 T^4 (N^2 - 1)/24$ in the present case. We focus in this part on the temperature range $(1-5) T_c$, that should correspond to the strongly coupled phase of the gluon-gluino plasma. The full SU(3) pressure is displayed in Fig. 1 and decomposed into the free gas, scattering and bound state parts. The free part is given by

$$\Omega_0 = 2(N^2 - 1) [\omega_+(m_g) + \omega_-(m_{\tilde{g}})], \quad (28)$$

with $m_g = m_{\tilde{g}}$. For the scattering and the bound state parts, according to the selection criterion given in Sec. II D, all possible color channels and all helicity channels with $\langle \vec{L}^2 \rangle \leq 5$ (except $|S_-; 1^+ \{4\}\rangle$ and $|D_-; 2^- \{4\}\rangle$ gg states) are included in the computation (see Appendices A and B).

The global structure has the same features as previously observed in the ordinary YM case [5]. The bound-state contribution is weak at every computed temperature but it is logically maximal around $1.2 T_c$, where the trace anomaly appears to be maximal (see Fig. 3). The scattering part is also maximal around $1.2 T_c$. At higher temperatures the repulsive gg channel $(2, 0, \dots, 0, 2)$ is dominant in the scattering part and tends to decrease the free gas part. Nevertheless, the effect of two-body interactions on the pressure is a minor contribution to the total pressure. This validates the use of the virial expansion (1) for which deviations from the ideal gas of massive particles must be weak. The slight differences between the ordinary YM and the $\mathcal{N} = 1$ SUSY YM are: The bound state sector is richer since $\tilde{g}\tilde{g}$, and $g\tilde{g}$ bound states exist up to $1.3 T_c$ in their most attractive channel, and the scattering part is naturally build with much more channels.

In Fig. 2, the SU(N) gauge structure of the normalized total pressure is shown. Again in this case, an asymptotically SU(N) gauge-group independent observable seems to emerge: The maximum deviation between the curves is just above T_c . This is in agreement with the scaling relations introduced in [5]. Indeed, if we expand the T -matrix in terms of V , the color dependence of the total pressure (without considering bound states) is in $\dim adj$ up to $O(V^3)$. This factor is thus cancelled by the same one in the pressure of normalization, and so the gauge-group independence is obtained at high temperature since such expansion

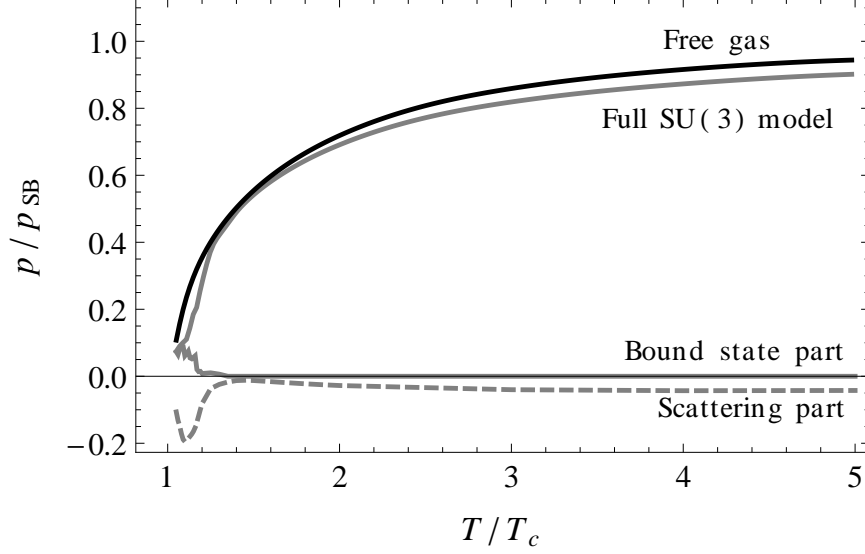


FIG. 1. Normalized pressure p/p_{SB} versus temperature in units of T_c , computed for the gauge group $SU(3)$. The full pressure is shown, together with the free gas, bound states and scattering contributions.

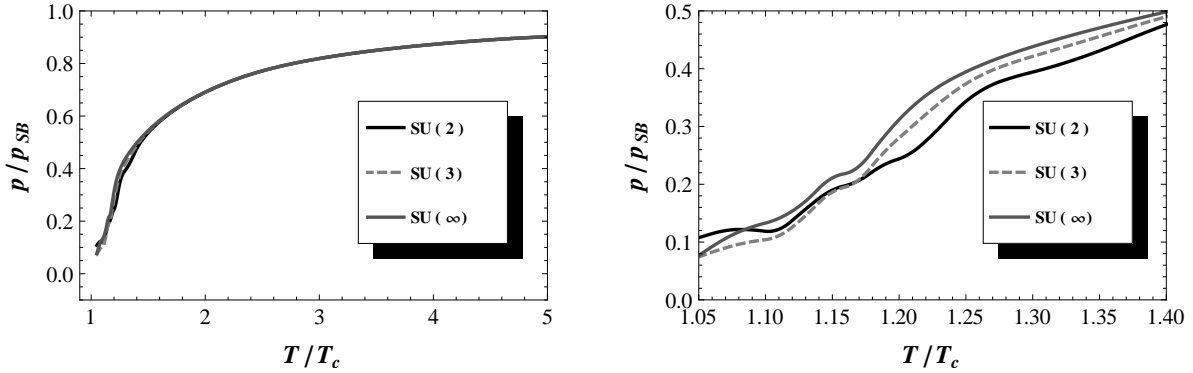


FIG. 2. (Left) Normalized pressure p/p_{SB} versus temperature in units of T_c , computed for different $SU(N)$ gauge groups. (Right) Zoom near T_c .

of the T -matrix becomes more and more valid with an increase of T . Moreover, it is worth adding that this extraction of the color factors is possible only because the gluon and gluino mass is gauge-group independent in our framework.

The behavior of the total normalized trace anomaly is displayed in Fig. 3. Again, we find appropriate to compute it without bound state (the treatment of bound states requires a more refined study [5]) and to compare it to the normalized free gas part Ω_0 . We also

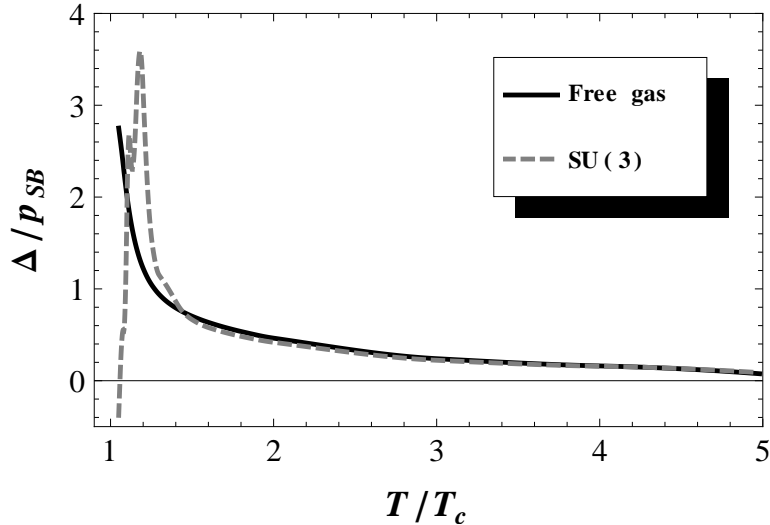


FIG. 3. Normalized trace anomaly Δ/p_{SB} versus temperature in units of T_c , compared to the normalized free gas part of Ω_0

observe in this case that the interactions provide the peak structure and that the trace anomaly tends to zero at high T ; the free part alone would not lead to this peak structure.

Finally, the last thermodynamic quantities we want to discuss in this section is the normalized trace anomaly for $SU(N)$ groups, presented in Fig. 4. The asymptotic gauge-group universality is, without surprise, observed and follows the same justification as the normalized pressure. The behavior around T_c exhibits some slight differences according to the gauge group. This can be understood by the fact that the number of channels to include in the computation depends on it.

B. Comparison with ordinary YM theory

At this stage it is natural to wonder whether the inclusion of fermions has a strong impact or not on the EoS compared to ordinary YM theory. In other words: How far the EoS of the supersymmetric and non supersymmetric cases are? Since our framework has already proven to describe in a satisfactory manner the lattice EoS of ordinary YM theory with gauge groups $SU(N)$ [5], we are in position to compare these previous results with the new ones. Recall that the comparison between the SUSY and non-SUSY cases is done for a constant ratio $T_c/\sqrt{\sigma}$ so that the dynamical effects due to the inclusions of fermions appear

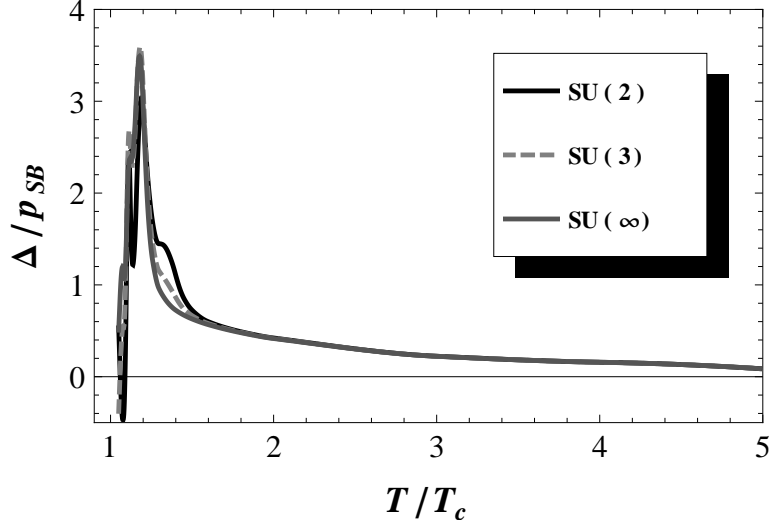


FIG. 4. Normalized trace anomaly Δ/p_{SB} versus temperature in units of T_c for different $SU(N)$ gauge groups.

more clearly. This is done in Fig. 5. It is readily seen that adding the gluinos significantly increases the normalized pressure. This is due to the fact that gluinos are both fermionic and in the adjoint representation. Hence, their contribution is of the same order than the gluons, not as in standard QCD. Moreover, it is worth noticing that the normalization is not the same in ordinary YM and $\mathcal{N} = 1$ SUSY YM since one and two species are involved respectively.

C. High temperatures

The interaction potential progressively vanishes at high temperatures because of the increasing screening. Consequently the high temperature limit of our model should be accurately described within the Born approximation $\mathcal{T} = V + \mathcal{O}(V^2)$. It has been shown in [5] that the interactions between two different species vanish within this approximation because of an identity relating the color factors: $\sum_{\mathcal{C}} \dim \mathcal{C} \kappa_{\mathcal{C},ij} = 0$. This sum actually appears when summing the different color contribution to the grand potential of a given channel involving two different species. When two identical species are involved, this argument does not hold because the summation is restricted to channels with a given symmetry.

In conclusion, gluons and gluinos do not interact with each other at high temperature in

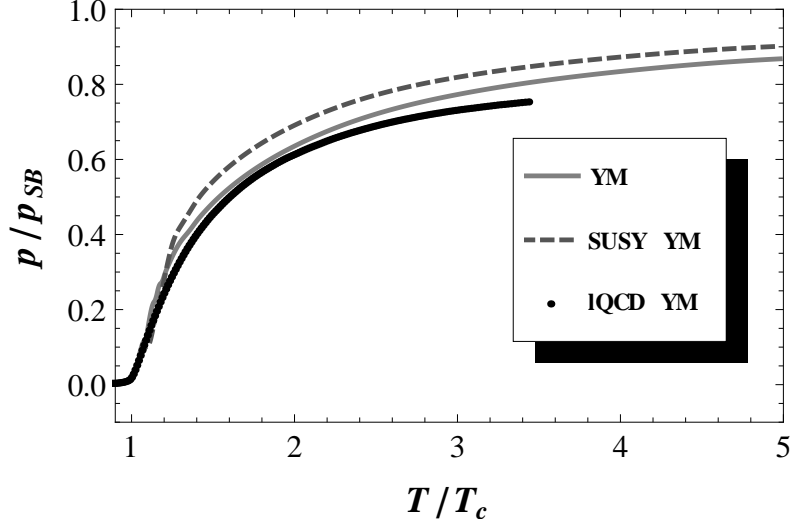


FIG. 5. Normalized pressure p/p_{SB} versus temperature in units of T_c for the gauge group $SU(3)$ in the $\mathcal{N} = 1$ SUSY YM case (dashed line) and ordinary YM case (solid line). Lattice data of [35] corresponding to the ordinary $SU(3)$ YM case are also indicated for comparison (dots).

average. However, the interactions between gluons only and gluinos only are still present.

V. ORIENTIFOLD EQUIVALENCE

Let us denote by QCD_{AS} a $SU(N)$ YM theory with N_f Dirac fermions in the two-index antisymmetric representation $(0, 1, 0, \dots, 0)$, and QCD_{adj} an $SU(N)$ YM theory with N_f Majorana flavors in the adjoint representation. The so-called orientifold equivalence states that QCD_{AS} and QCD_{adj} are equivalent at large N in the bosonic sector [19]. This equivalence is particularly appealing when $N_f = 1$ since in this case QCD_{adj} is actually $\mathcal{N} = 1$ SUSY YM. Moreover, QCD_{AS} reduces to standard one-flavor QCD ($I = 0$) for $N = 3$.

Within our framework it is possible to show that orientifold equivalence holds, and to compute how far one-flavor QCD deviates for the large- N limit. This is the purpose of the present section where we notice that the meaning of the symbol \cong will be “equal at the limit $N \rightarrow \infty$ ”. Moreover, q_A (\bar{q}_A) will denote a(n) (anti)quark in the two-index antisymmetric representation. Possible color channels pairs containing q_A or \bar{q}_A are given in Appendix A, and helicity channels in Appendix B.

First, we have to check that the masses of the particles coincide. The gluon thermal mass

is common to QCD_{AS} and QCD_{adj} since the gluonic sector is identical in both theories. An assumption of our model is that the function $\Delta(T)$ is gauge-group independent. Hence, $\delta_{\tilde{g}}(T) = \delta_g(T) = \Delta(T)$. Using the color factors listed in Appendix A, one gets

$$\delta_{q_A}(T) = \delta_{\bar{q}_A}(T) = \sqrt{\frac{N^2 - N - 2}{N^2}} \Delta(T) \quad (29)$$

which is not equal to $\Delta(T)$ in general. Nevertheless, $\delta_{q_A}(T) = \delta_{\bar{q}_A}(T) \cong \delta_{\tilde{g}}(T)$ as expected. To obtain the equality between the thermal masses $m_{\tilde{g}}$, m_{q_A} and $m_{\bar{q}_A}$ at large N , it is necessary to take the same value of the parameter m_0 for the three particles (a study with physical quark masses will be presented elsewhere [36]). As m_0 is assumed to be gauge-group-independent, this parameter is constant with N . The free gluinos thus bring a contribution $\Omega_0(\tilde{g}) = 2(N^2 - 1)\omega_-(m_{\tilde{g}})$ to the grand potential, while the free quarks and antiquarks bring a corresponding contribution $\Omega_0(q_A, \bar{q}_A) = 2\frac{N(N-1)}{2}\omega_-(m_{q_A}) + 2\frac{N(N-1)}{2}\omega_-(m_{\bar{q}_A})$. It is then straightforwardly checked that

$$\Omega_0(\tilde{g}) \cong \Omega_0(q_A, \bar{q}_A). \quad (30)$$

After the equivalence of the free part, we have to show the equivalence of the two-body contributions. The gg channels are trivially equal in QCD_{AS} and QCD_{adj} , so only the $\tilde{g}\tilde{g}$ and $\tilde{g}g$ channels have to be investigated.

The $\tilde{g}\tilde{g}$ channels are bosonic; their contribution should thus be equivalent to that of the $q_A q_A$, $\bar{q}_A \bar{q}_A$ and $\bar{q}_A q_A$ ones. The color singlet appears in $\tilde{g}\tilde{g}$ and $q_A \bar{q}_A$; the corresponding contributions to the pressure are different because the Pauli principle has to be applied in the first one, not in the second one. This discrepancy is irrelevant at large N because the singlet's contribution is of order 1, not N^2 . The symmetric and antisymmetric adjoint channels in $\tilde{g}\tilde{g}$ bring a pressure contribution which is equal to the adjoint channel appearing in $q_A \bar{q}_A$: All the possible helicity states are allowed in both cases. The $(2, 0, \dots, 1, 0)$ and $(0, 1, \dots, 0, 2)$ channels in $\tilde{g}\tilde{g}$ have no equivalent in the quark case, but they bring no contribution to the EoS since $\kappa_C = 0$. The remaining color channels in $\tilde{g}\tilde{g}$ are the symmetric $(2, 0, \dots, 0, 2)$ and $(0, 1, \dots, 1, 0)$ ones, that should match with the symmetric $(0, 0, 0, 1, 0, \dots, 0)$ and $(0, \dots, 0, 1, 0, 0, 0)$ ones in $q_A q_A$ and $\bar{q}_A \bar{q}_A$. This is actually the case. Indeed, Pauli principle asks the $\tilde{g}\tilde{g}$ states to have $L + S$ even, just as for the $q_A q_A$ and $\bar{q}_A \bar{q}_A$ states. Moreover, the Born approximation is valid at large N for all those channels since $\kappa_C = O(1/N)$. The contributions of the $\tilde{g}\tilde{g}$ channels to the grand potential is thus proportional to $\sum_C \dim \mathcal{C} \kappa_C = (N^2 - 1)/2$, as well as the $q_A q_A$, $\bar{q}_A \bar{q}_A$, $q_A \bar{q}_A$ ones for which

$\sum_{\mathcal{C}} \dim \mathcal{C} \kappa_{\mathcal{C}} + \sum_{\bar{\mathcal{C}}} \dim \bar{\mathcal{C}} \kappa_{\bar{\mathcal{C}}} = (N^2 - 1)(N - 2)/(2N)$. Both factors are equal at large N , leading to equivalent contributions to the EoS.

Finally, the $\tilde{g}g$ contribution should be equivalent to the q_{Ag} and \bar{q}_{Ag} ones. The same kind of arguments apply, so we will not perform the full analysis for the sake of clarity. Let us just mention that the two adjoint channels in $\tilde{g}g$ bring equivalent contributions to the grand potential than the $(2, 0, \dots, 0)$ and $(0, 1, 0, \dots, 0)$ channels in q_{Ag} and \bar{q}_{Ag} . Similarly, the $(2, 0, \dots, 0, 2)$ and $(0, 1, \dots, 1, 0)$ channels in $\tilde{g}g$ match with the $(1, 1, 0, \dots, 0, 1)$ and $(0, 0, 1, 0, \dots, 0, 1)$ one in q_{Ag} and \bar{q}_{Ag} .

The above discussion shows that $\text{QCD}_{AS} \cong \text{QCD}_{adj}$: The orientifold equivalence is checked within our framework. This can be seen as a strong validation of the various assumptions made in the building of the model. Now we can compare the accuracy of the orientifold equivalence at finite N , namely $N = 3$. The pressure and trace anomaly of $\text{SU}(3)$ $\mathcal{N} = 1$ SUSY YM is compared to the EoS of $\text{SU}(3)$ one-flavor QCD in Fig. 6. The free part is given by, for $\text{SU}(N)$ gauge groups,

$$\Omega_0 = 2(N^2 - 1)\omega_+(m_g) + 2N(N - 1)\omega_-(m_{q_A}). \quad (31)$$

For the scattering and the bound state parts, according to the selection criterion given in Appendix D, all possible color channels and all helicity channels with $\langle \vec{L}^2 \rangle \leq 5$ (except $|S_-; 1^+ \{4\}\rangle$ and $|D_-; 2^- \{4\}\rangle$ gg states) are included in the computation. These plots show how far one-flavor QCD is from the $\mathcal{N} = 1$ SUSY YM theory at the level of the EoS. As far as the pressure is concerned, both theories are very similar. The trace anomaly however reveals some differences around $1.2 T_c$. Note that each case is normalized to its own Stefan-Boltzmann pressure, that of QCD_{AS} reading $p_{SB} = \pi^2 T^4 (N - 1)(\frac{15}{8}N + 1)/45$ for $\text{SU}(N)$ gauge groups..

VI. CONCLUSIONS

We have studied the properties of the deconfined phase of $\mathcal{N} = 1$ SUSY YM with a T -matrix formulation that had already proven to be successful in the modeling of ordinary YM theory. Here is a summary of the results we have found:

- Among the various possible bound states, the $a - \eta'$, the scalar glueball and the lightest gluino-gluon bound state can survive up to $1.3 T_c$, implying that the gluon-gluino

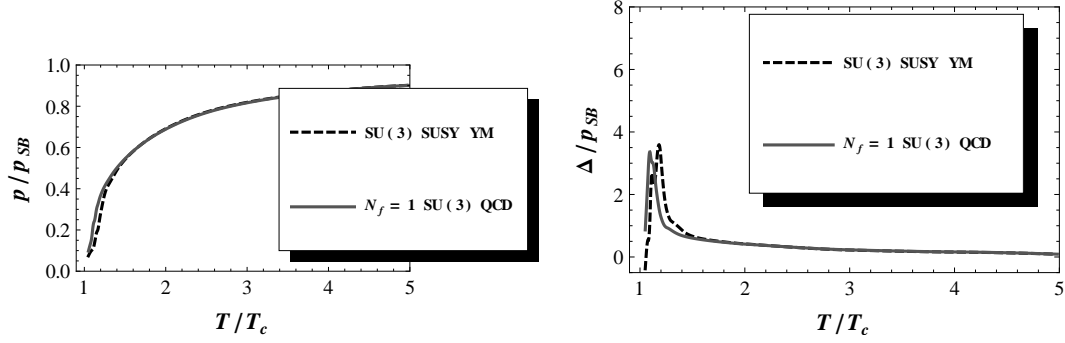


FIG. 6. (Left) Normalized pressure p/p_{SB} versus temperature in units of T_c , computed for SU(3) QCD with $N_f = 1$ and $\mathcal{N} = 1$ SU(3) SUSY YM. (Right) Normalized trace anomaly Δ/p_{SB} versus temperature in units of T_c , computed for SU(3) QCD with $N_f = 1$ and $\mathcal{N} = 1$ SU(3) SUSY YM.

plasma is rich in bound states in the temperature range where the trace anomaly is maximal. Its non-ideality is thus clearly related to the strength of the interactions, which are strong enough to create bound states.

- The bound-state properties are independent of the number of colors in the singlet channel, and the normalized EoS is only weakly dependent on the number of colors for the gauge groups SU(N). The EoS is also slightly above the non-supersymmetric case, at least when keeping $T_c/\sqrt{\sigma}$ constant.
- At large temperatures, the trace anomaly decreases as expected from the β -function, and the two-body gluon-gluino interactions are suppressed while it is not the case for the gluon-gluon and gluino-gluino interactions.
- The orientifold duality holds at the level of the EoS within our formalism. Some differences exist between one-flavor QCD and SU(3) $\mathcal{N} = 1$ SUSY YM at the level of the trace anomaly. Such a disagreement is not unexpected since the duality is exact at large- N only.

We have focused here on SU(N) gauge groups for the study of the EoS for a gluon-gluino gas. However, our formalism can be implemented for any gauge group. We expect that the dependence of the EoS on the gauge group should be weak because the dominant contribution to the EoS appears to be the free part, which is gauge-group independent once

normalized to the Stefan-Boltzmann pressure. The problem is nevertheless worth to be studied and is left for future works, as well as the extension of our formalism to a larger number of supersymmetries.

All results are obtained here for a fixed value of $T_c = 0.3$ GeV (more precisely for a fixed value of $T_c/\sqrt{\sigma}$, as explained in [5]). As mentioned above, T_c might be approximately 20% lower in the case under study than in ordinary YM theory [16]. Moreover, when quarks enters into the game, a value around 0.15 GeV is expected [37]. So, a study of the behavior of the thermodynamic observables as a function of T_c in our model is worth to perform. Such a work is in progress [36].

ACKNOWLEDGMENTS

G. L. thanks the F.R.S-FNRS for financial support.

Appendix A: Two-body color channels for $SU(N)$

Characteristics of color channels for particles in the adjoint representation of $SU(N)$ can be found in [5], but they are recalled here in Table III for completeness: condition of existence as a function of N , possible symmetry (Symmetrical or Antisymmetrical), dimension and color factor ($\kappa_{\mathcal{C}}$ defined in (6)). Characteristics of color channels, implying a particle in the antisymmetrical $(0, 1, 0, \dots, 0)$ representation of $SU(N)$, are given in Table IV-VI. One can check that $\sum_{\mathcal{C}} \dim \mathcal{C} = \dim R_1 \times \dim R_2$ and $\sum_{\mathcal{C}} \dim \mathcal{C} \kappa_{\mathcal{C},12} = 0$. Note that a general method for computing the quadratic Casimir of $SU(N)$ can be found in [38].

TABLE III. Condition of existence, symmetry, dimension and color factor ($\kappa_{\mathcal{C}}$) of the color channels (\mathcal{C}) appearing in the tensor products of $g g$ channels, where g is the adjoint representation of $SU(N)$.

\mathcal{C}	• $(1, 0, \dots, 0, 1) (2, 0, \dots, 0, 2) (2, 0, \dots, 1, 0) (0, 1, 0, \dots, 0, 1, 0) (0, 1, \dots, 2)$				
$N \geq$	2	3(S),2(A)	2	3	4
Symmetry	S	S,A	S	A	S
Dimension	1	$N^2 - 1$	$\frac{N^2(N+3)(N-1)}{4}$	$\frac{(N^2-4)(N^2-1)}{4}$	$\frac{N^2(N-3)(N+1)}{4}$
$\kappa_{\mathcal{C}}$	-1	$-\frac{1}{2}$	$\frac{1}{N}$	0	$-\frac{1}{N}$

TABLE IV. Same as Table III, but for the tensor products of $q_A q_A$, where q_A is the antisymmetrical $(0, 1, 0, \dots, 0)$ representation of $SU(N)$ with dimension $N(N-1)/2$. For each $q_A q_A$ channel \mathcal{C} , a $\bar{q}_A \bar{q}_A$ channel $\bar{\mathcal{C}}$ exists with the same characteristics.

\mathcal{C}	$(0, 2, 0, \dots, 0)$	$(1, 0, 1, 0, \dots, 0)$	$(0, 0, 0, 1, 0, \dots, 0)$
$\bar{\mathcal{C}}$	$(0, \dots, 0, 2, 0)$	$(0, \dots, 0, 1, 0, 1)$	$(0, \dots, 0, 1, 0, 0, 0)$
$N \geq$	2	3	4
Symmetry	S	A	S
Dimension	$\frac{N^2(N^2-1)}{12}$	$\frac{N(N^2-1)(N-2)}{8}$	$\frac{N(N-1)(N-2)(N-3)}{24}$
$\kappa_{\mathcal{C}}$	$\frac{N-2}{N^2}$	$-\frac{2}{N^2}$	$-\frac{2(N+1)}{N^2}$

TABLE V. Same as Table III, but for $q_A \bar{q}_A$ channels.

\mathcal{C}	\bullet	$(1, 0, \dots, 0, 1)$	$(0, 1, 0, \dots, 0, 1, 0)$
$N \geq$	2	3	4
Dimension	1	$N^2 - 1$	$\frac{(N-3)N^2(N+1)}{4}$
$\kappa_{\mathcal{C}}$	$-\frac{(N-2)(N+1)}{N^2}$	$\frac{-N^2+2N+4}{2N^2}$	$\frac{2}{N^2}$

TABLE VI. Same as Table III, but for $q_A g$ channels. For each $q_A g$ channel \mathcal{C} , a $\bar{q}_A g$ channel $\bar{\mathcal{C}}$ exists with the same characteristics.

\mathcal{C}	$(2, 0, \dots, 0)$	$(0, 1, 0, \dots, 0)$	$(1, 1, 0, \dots, 0, 1)$	$(0, 0, 1, 0, \dots, 0, 1)$
$\bar{\mathcal{C}}$	$(0, \dots, 0, 2)$	$(0, \dots, 0, 1, 0)$	$(1, 0, \dots, 0, 1, 1)$	$(1, 0, \dots, 0, 1, 0, 0)$
$N \geq$	2	3	3	4
Dimension	$\frac{N(N+1)}{2}$	$\frac{N(N-1)}{2}$	$\frac{N^2(N^2-4)}{3}$	$\frac{N(N^2-1)(N-3)}{6}$
$\kappa_{\mathcal{C}}$	$-\frac{N-2}{2N}$	$-\frac{1}{2}$	$\frac{1}{2N}$	$-\frac{1}{N}$

Appendix B: Helicity formalism for spin-1/2 and transverse spin-1 particles

The proper way to manage two-body states containing gluons, gluinos or quarks is to use the Jacob and Wick's helicity formalism [26], since a gluon is a transverse spin-1 particle and a quark or a gluino is a spin-1/2 particle. A two-body state with total spin J , with

helicities λ_1 and λ_2 , and with a given parity P can be written

$$|J^P, M; \lambda_1, \lambda_2, \epsilon\rangle = \frac{1}{\sqrt{2}} [|J, M; \lambda_1, \lambda_2\rangle + \epsilon |J, M; -\lambda_1, -\lambda_2\rangle], \quad (\text{B1})$$

with $\epsilon = \pm 1$ and $|J, M; \lambda_1, \lambda_2\rangle$ a two-particle helicity state in the rest frame of the system. The parity is given by $P = \epsilon \eta_1 \eta_2 (-1)^{J-s_1-s_2}$ with η_i and s_i the intrinsic parity and spin of particle i . Moreover, $J \geq |\lambda_1 - \lambda_2|$. The helicity states can be expressed as particular linear combinations of usual normalized basis states $|^{2S+1}L_J\rangle$, which is very convenient to perform the computations [26]

$$|J, M; \lambda_1, \lambda_2\rangle = \sum_{L,S} \left[\frac{2L+1}{2J+1} \right]^{1/2} \langle L, S; 0, \lambda_1 - \lambda_2 | J, \lambda_1 - \lambda_2 \rangle \times \langle s_1, s_2; \lambda_1, -\lambda_2 | S, \lambda_1 - \lambda_2 \rangle |^{2S+1}L_J\rangle. \quad (\text{B2})$$

For the present work, it is sufficient to recall that four families of helicity states can be found, separated in helicity singlets $|S_{\pm}; J^P\rangle$ ($\lambda_1 \lambda_2 > 0$) and doublets $|D_{\pm}; J^P\rangle$ ($\lambda_1 \lambda_2 < 0$), with $\epsilon = \pm 1$. This notation follows the pioneering work [39] and is used in [40]. In the special case of identical particles, the helicity states must also be eigenstates of the operator $\hat{\mathcal{S}} = [1 + (-1)^{2s} P_{12}]$, which is the projector on the symmetric (s integer) or antisymmetric (s half-integer) part of the helicity state. It can be seen that the states [40]

$$|J^P, M; \lambda_1, \lambda_2, \epsilon, \rho\rangle = \frac{1}{2} \{ |J^P, M; \lambda_1, \lambda_2, \epsilon\rangle + \rho |J^P, M; \lambda_2, \lambda_1, \epsilon\rangle \}, \quad (\text{B3})$$

with $\rho = \pm 1$, are eigenstates of $\hat{\mathcal{S}}$ with the eigenvalues $1 + \rho(-1)^J$.

1. Two transverse spin-1 particles

The general forms of the two-gluon states have been presented in [40]. Some properties are given in Table VII, as well as the average value of some operators, computed with these states. For completeness, the ones considered in this paper are recalled here.

The number between braces being the value of $\langle \vec{L}^2 \rangle$, the first symmetric states are:

$$|S_+; 0^+ \{2\}\rangle = \left[\frac{2}{3} \right]^{1/2} |^1S_0\rangle + \left[\frac{1}{3} \right]^{1/2} |^5D_0\rangle, \quad (\text{B4})$$

$$|S_-; 0^- \{2\}\rangle = -|^3P_0\rangle, \quad (\text{B5})$$

$$|D_+; 2^+ \{4\}\rangle = \left[\frac{2}{5} \right]^{1/2} |^5S_2\rangle + \left[\frac{4}{7} \right]^{1/2} |^5D_2\rangle + \left[\frac{1}{35} \right]^{1/2} |^5G_2\rangle. \quad (\text{B6})$$

TABLE VII. Symmetrized (S) and antisymmetrized (A) two-gluon helicity states, following the notation of [39, 40], with the corresponding quantum numbers and some averaged operators.

State	S	A	$\langle \vec{L}^2 \rangle$	$\langle \vec{S}^2 \rangle$	$\langle \vec{L} \cdot \vec{S} \rangle$
$ S_+; J^P\rangle$	(even- $J \geq 0$) ⁺	(odd- $J \geq 1$) ⁻	$J(J+1)+2$	2	-2
$ S_-; J^P\rangle$	(even- $J \geq 0$) ⁻	(odd- $J \geq 1$) ⁺	$J(J+1)+2$	2	-2
$ D_+; J^P\rangle$	(even- $J \geq 2$) ⁺	(odd- $J \geq 3$) ⁻	$J(J+1)-2$	6	-2
$ D_-; J^P\rangle$	(odd- $J \geq 3$) ⁺	(even- $J \geq 2$) ⁻	$J(J+1)-2$	6	-2

The first antisymmetric states are:

$$|S_+; 1^-\{4\}\rangle = \left[\frac{2}{3}\right]^{1/2} |^1P_1\rangle - \left[\frac{2}{15}\right]^{1/2} |^5P_1\rangle + \left[\frac{1}{5}\right]^{1/2} |^5F_1\rangle, \quad (\text{B7})$$

$$|S_-; 1^+\{4\}\rangle = \left[\frac{1}{3}\right]^{1/2} |^3S_1\rangle - \left[\frac{2}{3}\right]^{1/2} |^3D_1\rangle, \quad (\text{B8})$$

$$|D_-; 2^-\{4\}\rangle = -\left[\frac{4}{5}\right]^{1/2} |^5P_2\rangle - \left[\frac{1}{5}\right]^{1/2} |^5F_2\rangle. \quad (\text{B9})$$

All other states are characterized by $\langle \vec{L}^2 \rangle \geq 8$; their general form can be found in [40].

2. States containing one transverse spin-1 particle

States containing a gluon and a gluino or a quark can also be expressed as particular linear combinations of usual basis states $|^{2S+1}L_J\rangle$, following the procedure given in [40]. Some properties are given in Table VIII, as well as the average value of some operators, computed with these states.

TABLE VIII. Helicity states containing a gluon and a gluino or a quark, following the notation of [39, 40], with the corresponding quantum numbers and some averaged operators.

State	J min	$\langle \vec{L}^2 \rangle$	$\langle \vec{S}^2 \rangle$	$\langle \vec{L} \cdot \vec{S} \rangle$
$ S_{\pm}; J^P\rangle$	$\frac{1}{2}$	$J(J+1) + \frac{5}{4}$	$\frac{7}{4}$	$-\frac{3}{2}$
$ D_{\pm}; J^P\rangle$	$\frac{3}{2}$	$J(J+1) - \frac{3}{4}$	$\frac{15}{4}$	$-\frac{3}{2}$

The general forms of the qg states read as

$$\begin{aligned} \left| S_+; J^{(-1)^{j-1/2}} \right\rangle &= \left[\frac{2J-1}{8J} \right]^{1/2} \left| {}^4J-3/2_J \right\rangle + \left[\frac{2}{3} \right]^{1/2} \left| {}^2J+1/2_J \right\rangle \\ &\quad - \left[\frac{2J+3}{24J} \right]^{1/2} \left| {}^4J+1/2_J \right\rangle, \end{aligned} \quad (\text{B10})$$

$$\begin{aligned} \left| S_-; J^{(-1)^{j+1/2}} \right\rangle &= \left[\frac{2}{3} \right]^{1/2} \left| {}^2J-1/2_J \right\rangle + \left[\frac{2J-1}{24(J+1)} \right]^{1/2} \left| {}^4J-1/2_J \right\rangle \\ &\quad - \left[\frac{2J+3}{8(J+1)} \right]^{1/2} \left| {}^4J+3/2_J \right\rangle, \end{aligned} \quad (\text{B11})$$

$$\left| D_+; J^{(-1)^{j-1/2}} \right\rangle = \left[\frac{2J+3}{8J} \right]^{1/2} \left| {}^4J-3/2_J \right\rangle + \left[\frac{3(2J-1)}{8J} \right]^{1/2} \left| {}^4J+1/2_J \right\rangle, \quad (\text{B12})$$

$$\left| D_-; J^{(-1)^{j+1/2}} \right\rangle = - \left[\frac{3(2J+3)}{8(J+1)} \right]^{1/2} \left| {}^4J-1/2_J \right\rangle - \left[\frac{2J-1}{8(J+1)} \right]^{1/2} \left| {}^4J+3/2_J \right\rangle. \quad (\text{B13})$$

The first qg states are $\left| S_+; \frac{1}{2}^+ \{2\} \right\rangle$, $\left| S_-; \frac{1}{2}^- \{2\} \right\rangle$, $\left| D_+; \frac{3}{2}^- \{3\} \right\rangle$, $\left| D_-; \frac{3}{2}^+ \{3\} \right\rangle$, $\left| S_+; \frac{3}{2}^- \{5\} \right\rangle$, $\left| S_-; \frac{3}{2}^+ \{5\} \right\rangle$. All other states are characterized by $\langle \tilde{L}^2 \rangle \geq 8$. The parity is reversed for $\bar{q}g$ states. It is not relevant for $\tilde{g}g$ states [41].

3. States containing only spin-1/2 particles

The particle-pairs $\tilde{g} \tilde{g}$, $q_A q_A$, $\bar{q}_A \bar{q}_A$, and $q_A \bar{q}_A$ are represented by ordinary states $|^{2S+1}L_J\rangle$. Let us point out that $\langle \tilde{L}^2 \rangle = 0, 2, 6$ for $L = 0, 1, 2$, respectively. So, we have considered all states with different values of J and S , compatible with $L \leq 1$.

Appendix C: Formulas for two different particles

Various formulas to compute the T -matrix and the scattering part of the pressure are given in [5], but only for two identical particles. We give here the corresponding relations for different masses. For two masses m_1 and m_2 , the asymptotical relative momentum \vec{q} is related to the center of mass energy E by $E = \epsilon_1(q) + \epsilon_2(q)$ with $\epsilon_i = \sqrt{\vec{q}^2 + m_i^2}$, which implies that

$$q(E) = \frac{\sqrt{(E^2 - (m_1 + m_2)^2)(E^2 - (m_1 - m_2)^2)}}{2E}. \quad (\text{C1})$$

One can check that

$$\epsilon_1(E) = \frac{E^2 + m_1^2 - m_2^2}{2E}, \quad (\text{C2})$$

with $\epsilon_2(E)$ given by permuting 1 and 2 in the above formula. These quantities are useful to compute the in-medium effects, namely the Bose-enhancement and the Pauli-blocking.

In the results shown below, the main difficulty is to take correctly into account the constraint (C1) into the various integrations on delta-distributions about energy and momentum conservations. As our interaction is spin-blind, we take for the two-body free propagator a spin-independent expression, in the same spirit as in [42]. Using the Blankenbecler-Sugar reduction scheme [43], we find

$$G_0(E; k) = m_1 m_2 \frac{\epsilon_1(k) + \epsilon_2(k)}{2\epsilon_1(k)\epsilon_2(k)} \frac{1}{\frac{E}{4} - \left(\frac{\epsilon_1(k) + \epsilon_2(k)}{2}\right)^2 + i(\Sigma_1 + \Sigma_2)}, \quad (\text{C3})$$

in agreement with [44] (the normalization is different in this last reference). The parameter $\Sigma_j = \Sigma_j^R + i\Sigma_j^I$ takes into account the gluon self-interaction. As in [5], we take $\Sigma_j^I = -0.01$ GeV for numerical purposes, and $\Sigma_j^R = 0$ since the real part can be reabsorbed in the effective gluon mass. We have checked that that our results are very similar by using the propagator in the Thompson scheme [45], in agreement with the results of [37].

Introducing the notation

$$\Lambda(E) = \frac{E^4 - (m_1^2 - m_2^2)^2}{E^3}, \quad (\text{C4})$$

the scattering part of (1) reads,

$$\begin{aligned} \Omega_s = & \frac{1}{64\pi^5\beta^2} \sum_I (2I+1) \sum_{J^P} (2J+1) \sum_{\mathcal{C}} \dim \mathcal{C} \\ & \times \left(\beta \int_{m_1+m_2}^{\infty} d\epsilon \epsilon^2 q(\epsilon) \Lambda(\epsilon) K_1(\beta\epsilon) \text{Re} \mathcal{T}_{J^P}(\epsilon; q(\epsilon), q(\epsilon)) \right. \\ & - \frac{1}{16\pi^2} \int_{m_1+m_2}^{\infty} d\epsilon \epsilon^2 q(\epsilon)^2 \Lambda(\epsilon)^2 K_2(\beta\epsilon) \text{Re} \mathcal{T}_{J^P}(\epsilon; q(\epsilon), q(\epsilon)) \text{Im} \mathcal{T}'_{J^P}(\epsilon; q(\epsilon), q(\epsilon)) \\ & \left. + \frac{1}{16\pi^2} \int_{m_1+m_2}^{\infty} d\epsilon \epsilon^2 q(\epsilon)^2 \Lambda(\epsilon)^2 K_2(\beta\epsilon) \text{Re} \mathcal{T}'_{J^P}(\epsilon; q(\epsilon), q(\epsilon)) \text{Im} \mathcal{T}_{J^P}(\epsilon; q(\epsilon), q(\epsilon)) \right) \quad (\text{C5}) \end{aligned}$$

where the symbol “prime” is the derivative respective to the energy.

Appendix D: Cross section

Using the formalism of [46], but adapted for a relativistic kinematics, it can be shown that the differential elastic cross section for a two-body interaction is given by

$$\frac{d\sigma}{d\Omega}(\vec{p} \leftarrow \vec{p}_0) = (2\pi)^4 \mu(E)^2 |\langle \vec{p} | \mathcal{T}(E + i0) | \vec{p}_0 \rangle|^2, \quad (\text{D1})$$

where $|\vec{p}_0| = |\vec{p}|$ and where $\mu(E) = \Lambda(E)/4$ (C4). The matrix element is evaluated for a given color-isospin channel. As expected, in the nonrelativistic limit, $\mu(E)$ tends to the reduced mass. By integration on the angles, one obtains

$$\sigma = (2\pi)^5 \mu(E)^2 \int_{-1}^{+1} d(\hat{p} \cdot \hat{p}_0) |\langle \vec{p} | \mathcal{T}(E + i0) | \vec{p}_0 \rangle|^2. \quad (\text{D2})$$

The ket $|\vec{p}\rangle$ is a plane wave state containing all possible partial components. By decomposing this state into helicity states, we obtain the cross section σ_{JP} for a given color-isospin- J^P channel

$$\sigma_{JP} = 4\pi^3 \mu(E)^2 |\mathcal{T}_{JP}(E)|^2. \quad (\text{D3})$$

Our purpose is to compare the contributions from various channels to the grand potential at a given temperature for all possible values of the center of mass energy. So, we define a kind of mean cross section $\bar{\sigma}_{JP}$ by integrating (D3) on the energy,

$$\bar{\sigma}_{JP} = 4\pi^3 \int_{m_1+m_2}^{\infty} dE \mu(E)^2 |\mathcal{T}_{JP}(E)|^2 [1 \pm f^1(\epsilon_1(E))] [1 \pm f^2(\epsilon_2(E))]. \quad (\text{D4})$$

The in-medium effects are taken into account, depending on the bosonic or fermionic nature of the two interacting particles. Following (11) and (C3), when $E \rightarrow \infty$, we have

$$\mathcal{T}_{JP}(E; q, q') \rightarrow V_{JP}(q, q'). \quad (\text{D5})$$

In our model, $V_{JP}(q, q')$ is essentially the Fourier transform of a Yukawa interaction which behaves like q^{-2} . So, the mean cross section, which depends only on T , is finite since $|\mathcal{T}_{JP}(E)|^2 \sim E^{-4}$ when $E \gg m_1 + m_2$. We have decided to estimate the relative contributions of two channels J^P and $J'^{P'}$ by computing the ratios $\bar{\sigma}_{JP}/\bar{\sigma}_{J'^{P'}}$.

-
- [1] K. Yagi, T. Hatsuda and Y. Miake, *Quark-Gluon Plasma: From Big Bang to Little Bang* (Cambridge Monographs on Particle Physics, Nuclear Physics and Cosmology, Cambridge University Press, 2008).
 - [2] M. Pepe and U.-J. Wiese, Nucl. Phys. B **768**, 21 (2007).
 - [3] J. Braun, A. Eichhorn, H. Gies, and J. M. Pawłowski, Eur. Phys. J. C **70**, 689 (2010).
 - [4] A. Dumitru, Y. Guo, Y. Hidaka, C. P. K. Altes, and R. D. Pisarski, Phys. Rev. D **86**, 105017 (2012).

- [5] G. Lacroix, C. Semay, D. Cabrera, and F. Buisseret, Phys. Rev. D **87**, 054025 (2013).
- [6] H. B. Meyer, Phys. Rev. D **80**, 051502(R) (2009).
- [7] F. Buisseret and G. Lacroix, Phys. Lett. B **705**, 405 (2011).
- [8] A. Salam and J. A. Strathdee, Phys. Lett. B **51**, 353 (1974).
- [9] V. A. Novikov, M. A. Shifman, A. I. Vainshtein, and V. I. Zakharov, Nucl. Phys. B **229**, 381 (1983).
- [10] G. Veneziano and S. Yankielowicz, Phys. Lett. B **113**, 231 (1982); G. R. Farrar, G. Gabadadze, and M. Schwetz, Phys. Rev. D **58**, 015009 (1998).
- [11] I. Campos *et al.* [DESY-Münster Collaboration], Eur. Phys. J. C **11**, 507 (1999).
- [12] F. Farchioni and R. Peetz, Eur. Phys. J. C **39**, 87 (2005).
- [13] A. Feo, P. Merlatti, and F. Sannino, Phys. Rev. D **70**, 096004 (2004).
- [14] K. Demmouche, F. Farchioni, A. Ferling, I. Montvay, G. Münster, E. E. Scholz, and J. Wuiloud, Eur. Phys. J. C **69**, 147 (2010).
- [15] G. Bergner, I. Montvay, G. Münster, U. D. Özugurel, and D. Sandbrink, JHEP **1311**, 061 (2013).
- [16] G. Bergner, P. Giudice, G. Münster, S. Piemonte and D. Sandbrink, arXiv:1405.3180 [hep-lat].
- [17] M. M. Anber, E. Poppitz, and B. Teeple, arXiv:1406.1199 [hep-th].
- [18] D. Amati, K. Konishi, Y. Meurice, G. C. Rossi and G. Veneziano, Phys. Rep. **162**, 169 (1988).
- [19] A. Armoni, M. Shifman, and G. Veneziano, Phys. Rev. Lett. **91**, 191601 (2003).
- [20] D. Cabrera and R. Rapp, Phys. Rev. D **76**, 114506 (2007).
- [21] R. Dashen, S.-K. Ma, and H. J. Bernstein, Phys. Rev. **187**, 345 (1969).
- [22] O. Kaczmarek, F. Karsch, P. Petreczky, and F. Zantow, Phys. Lett. B **543**, 41 (2002).
- [23] H. Satz, hep-ph/0602245; V. V. Dixit, Mod. Phys. Lett. A **5**, 227 (1990).
- [24] A. Mocsy and P. Petreczky, Phys. Rev. D **73**, 074007 (2006).
- [25] J.-P. Blaizot, E. Iancu, and A. Rebhan, Phys. Lett. B **470**, 181 (1999); Phys. Rev. D **63**, 065003 (2001).
- [26] M. Jacob and G. C. Wick, Annals Phys. **7**, 404 (1959).
- [27] S. Pratt and W. Bauer, Phys. Lett. B **329**, 413 (1994).
- [28] M. I. Haftel and F. Tabakin, Nucl. Phys. A **158**, 1 (1970).
- [29] G. S. Bali, Phys. Rep. **343**, 1 (2001); C. Semay, Eur. Phys. J. A **22**, 353 (2004); M. Cardoso and P. Bicudo, Phys. Rev. D **78**, 074508 (2008).

- [30] O. Oliveira and P. Bicudo, J. Phys. G **38**, 045003 (2011).
- [31] J. M. Cornwall, Phys. Rev. D **26**, 1453 (1982).
- [32] D. Binosi and J. Papavassiliou, Phys. Rep. **479**, 1 (2009).
- [33] E. V. Shuryak and I. Zahed, Phys. Rev. D **70**, 054507 (2004).
- [34] X. -F. Meng, G. Li, Y. Chen, C. Liu, Y. -B. Liu, J. -P. Ma, and J. -B. Zhang, Phys. Rev. D **80**, 114502 (2009).
- [35] M. Panero, Phys. Rev. Lett. **103**, 232001 (2009).
- [36] G. Lacroix, C. Semay, and F. Buisseret, in preparation.
- [37] M. Mannarelli and R. Rapp, Phys. Rev. C **72**, 064905 (2005).
- [38] B. Lucini and M. Teper, Phys. Rev. D **64**, 105019 (2001).
- [39] T. Barnes, Z. Phys. C **10**, 275 (1981).
- [40] V. Mathieu, F. Buisseret, and C. Semay, Phys. Rev. D **77**, 114022 (2008); F. Buisseret, V. Mathieu, and C. Semay, Phys. Rev. D **80**, 074021 (2009).
- [41] J. Zuk, G. C. Joshi, and J. W. G. Wignall, Phys. Rev. D **28**, 1706 (1983).
- [42] K. Huggins and R. Rapp, Nucl. Phys. A **896**, 24 (2012).
- [43] R. Blankenbecler and R. Sugar, Phys. Rev. **142**, 1051 (1966).
- [44] H. Mineo, J. A. Tjon, K. Tsushima, and S. N. Yang, Phys. Rev. C **77**, 055203 (2008).
- [45] R. H. Thompson, Phys. Rev. D **1**, 110 (1970).
- [46] J. R. Taylor, *Scattering Theory. The Quantum Theory of Nonrelativistic Collisions* (Dover Publications, New York, 1972).